

Residual stresses in rolled and machined nickel alloy plates: synchrotron X-ray diffraction measurement and three-dimensional eigenstrain analysis

A M Korsunsky^{1*}, G M Regino¹, D P Latham¹, H Y Li², and M J Walsh³

¹Department of Engineering Science, University of Oxford, Oxford, UK

²Department of Metallurgy and Materials, University of Birmingham, Birmingham, UK

³Rolls-Royce plc, Derby, UK

The manuscript was received on 10 August 2006 and was accepted after revision for publication on 11 October 2006.

DOI: 10.1243/03093247JSA260

Abstract: Most engineering components made from wrought metallic alloys undergo complex sequences of manufacturing operations. These processing steps frequently include extrusion, forging, or rolling, followed by machining and heat treatment. Since such components will be subjected to service loading as part of engineering assemblies, their durability must be assessed using suitably reliable life prediction models. The present study is aimed at the investigation of a combination of experimental and modelling techniques that involves microstructural investigation, diffraction measurement of residual elastic strains, and finite element simulation of residual stress distributions.

Eigenstrain-based modelling approach to the analysis of processing-induced residual stresses has been previously presented in the two-dimensional approximation, i.e. under the assumption that the equivalent permanent plastic strain field induced by processing is equibiaxial. Several different formulations were considered and compared, including plane stress, plane strain, and three-dimensional models. In the present study a further development of the eigenstrain-based analysis approach that incorporates the experimental data obtained from synchrotron X-ray diffraction measurements of residual elastic strains in two complementary cross-sections of a forged and machined nickel superalloy plate is reported. The microstructure was assessed using electron backscattered diffraction, and near-surface residual stresses evaluated using laboratory X-ray diffraction. It is found that the results of fully three-dimensional formulation differ from two-dimensional approximations particularly in the vicinity of machined surfaces, having potentially significant implications for durability assessment and fatigue life models.

Keywords: synchrotron, X-ray diffraction, eigenstrain, finite elements, residual stress, inverse problem

1 INTRODUCTION

Most manufacturing processes, such as extrusion, forging, rolling, casting, quenching, and welding, lead to the introduction of microstructural inhomogeneities and permanent deformation into the workpiece. Considerable progress has been achieved in recent years in coupled microstructural and

thermomechanical numerical process modelling. For example, heat treatment and quench hardening are frequently accompanied by phase transformation and inhomogeneous plastic flow, leading to distortion and residual stress generation. This requires the development of sophisticated coupled models (see, for example, the review by Rohde and Jeppsson [1]). Long-range or macroscopic residual stresses may be predicted by process models with some success.

In practice, however, detailed knowledge of the complete range of system parameters and the entire processing history is rarely available. As an

*Corresponding author: Department of Engineering Science, University of Oxford, Parks Road, Oxford, Oxfordshire, OX1 3PJ, UK. email: alexander.korsunsky@eng.ox.ac.uk

example that has particular relevance to the present study, sheet manufacture by rolling accompanied by inhomogeneous deformation, resulting in plastic strains that are strongly dependent on local grain size and orientation, may be considered. This non-uniformity of stiffness and strength at grain level arises owing to crystal anisotropy. As a consequence, rolled sheet or forgings that are assumed to be stress free in fact contain residual stresses, at least at the mesoscopic or microscopic level. This effect is particularly noticeable in polycrystalline samples containing relatively large grains.

For the purpose of obtaining the net shape, rolled or forged billets are usually subjected to surface machining. Near-surface layers of material undergo localized plastic deformation that may be more or less severe, depending on the geometry of the cutting tool, and in particular the rake angle [2]. As a result of machining-induced plastic deformation, short-range near-surface residual stresses arise in components.

The system of residual stress state inherited by an engineering component from prior processing stages affects its deformation behaviour. Particular interest from an engineering design viewpoint must be placed on the interaction between residual stresses and fatigue durability. The influence is mutual, in that residual stresses affect fatigue life, but cyclic loading, in turn, leads to residual stress evolution and redistribution.

A systematic investigation of the consequences of processing must include microstructural investigations in order to identify the arrangement, shape, size and orientation of grains. This often helps to reveal areas of significant plastic deformation, where sources of residual stress are located. Furthermore, plastic deformation is often associated with grain reorientation and texture development. Therefore, the use of electron-microscope-based techniques, such as electron backscattered diffraction (EBSD) for microtexture and grain structure mapping is particularly useful.

Next, the residual elastic strain (RES) state within the object must be investigated. It is often discovered that RES is present on different length scales, e.g. near a sample surface owing to surface treatment such as peening, coating, or machining, and in the bulk of the sample owing to prior processing operations, e.g. forging. Probing these distributions at the appropriate spatial resolution requires the use of suitable tools, e.g. non-destructive high-energy X-ray or neutron diffraction for bulk measurement, and conventional laboratory X-ray diffraction in combination with layer removal for near-surface depth profiling.

Finally, the experimental RES data must be interpreted in order to reconstruct the complete residual stress state within the sample and to provide input for subsequent residual stress evolution and fatigue initiation modelling.

A viable approach to the analysis of residual stress effects involves experimental characterization of residual stresses, or residual elastic strains in an engineering component after all processing operations have been completed, and before the assembly is put into service. However, at this stage a difficulty associated with the fact that measured residual stress state may not be self-equilibrated or may in fact be known only at some selected locations within the component is frequently encountered. Furthermore, the introduction into numerical simulations of *initial stress* (rather than eigenstrain) within the finite element framework does not guarantee stress equilibrium. Even if the analytically prescribed initial stress distribution is self-equilibrated, the nature of its application by discrete sampling at finite element nodes is likely to disturb this equilibrium, causing further redistribution.

In order to overcome the above difficulties, the eigenstrain-based residual stress modelling framework has been proposed [3] which possesses several advantages. Firstly, it offers a natural and straightforward means of incorporating residual stresses within the finite element framework. Importantly, by the very nature of the formulation, any distribution of eigenstrains gives rise to a self-equilibrating residual stress state. Secondly, subsequent inelastic deformation occurring owing to plasticity or phase transformation can be readily accounted for. This leads to the modification of eigenstrain distribution, allowing the residual stress evolution to be modelled.

A previous study [4] focused on the two-dimensional approximation of the near-surface residual stress states in machined nickel superalloy plates. The two-dimensional approximation presents a clear limitation, since it disregards the difference between in-plane stress components longitudinal and transverse with respect to the cutting direction. Furthermore, in the previous study the plate was assumed to be free from permanent inelastic strain (eigenstrain) beyond the depth affected by cutting. The above discussion of prior processing by rolling or forging suggests that similar short-range residual stresses may in fact be present throughout the depth of the sheet and must be accounted for. These issues are addressed in the present paper.

The experimental procedure used for residual elastic strain measurement in the bulk of material is the diffraction of high-energy synchrotron X-rays.

Forward scattering of high-energy X-ray beams causes sampling volumes to be elongated in the direction of the incident beam, leading to a reduction in the spatial resolution in that direction. However, in directions perpendicular to the incident beam, very good resolution of a few tens of microns can be achieved without X-ray optics, purely by beam collimation.

The three-dimensional residual stress state in a machined plate is reconstructed from a series of residual elastic strain measurements carried out on two mutually orthogonal thin slices. The relationship is discussed between fully coupled three-dimensional reconstruction relying on the measurements in both slices, and two-dimensional analyses using single-slice data.

Complementary laboratory X-ray measurements of near-surface residual stresses were also undertaken. The results are analysed in order to identify the mechanisms of plastic deformation that act as the source of the residual stress state.

2 EIGENSTRAIN MODELLING

The relationship between the permanent inelastic strain (eigenstrain) ε^* present in the sample and the residual elastic strain e that arises by the process of stress equilibration exhibits a complex dependence on the sample geometry. However, a helpful fundamental feature of this relationship is its linearity. In other words, for a given eigenstrain distribution $\varepsilon_{ij}^*(\mathbf{x}')$, the corresponding residual elastic strain $e_{kl}(\mathbf{x})$ in an otherwise elastic body is expressed by the formula [5]

$$e_{kl}(\mathbf{x}) = -\varepsilon_{kl}^*(\mathbf{x}) - \int_{-\infty}^{\infty} C_{pqmn} \varepsilon_{mn}^*(\mathbf{x}') G_{kp,ql}(\mathbf{x} - \mathbf{x}') d\mathbf{x}' \quad (1)$$

Here C_{ijkl} are the elastic stiffness coefficients, and $G_{kp}(\mathbf{x} - \mathbf{x}')$ denotes the Green's function for the particular geometry. While this function is known explicitly for some special geometries (e.g. infinite space, semi-infinite space bounded by a plane, and the corresponding two-dimensional solution), it is not practicable to seek analytical expressions for $G_{kp}(\mathbf{x} - \mathbf{x}')$ for many geometries of applied interest, such as engineering components of complex shape. The main significance of equation (1) for the present discussion, then, lies in the fact that it provides an explicit statement of linear interdependence between $\varepsilon_{ij}^*(\mathbf{x}')$ and $e_{kl}(\mathbf{x})$.

The integral on the right-hand side of equation (1) can be restricted to the region where $\varepsilon_{ij}^*(\mathbf{x}') \neq 0$, since

it clearly can be evaluated to zero everywhere else. This integral is formally divergent, because the second derivative of the Green's function $G_{kp,ql}(\mathbf{x} - \mathbf{x}')$ appearing in the equation is hypersingular in terms of $|\mathbf{x} - \mathbf{x}'|$. To obtain a useful formulation the integral must be understood in the finite part sense [6].

In practice the incorporation of eigenstrains in objects of arbitrarily complex geometry and avoiding singularities in the formulation can be accomplished using finite element methods, using the methodology that has been introduced elsewhere [7]. Furthermore, it has been shown that an efficient approach can be developed for the determination of unknown eigenstrain distributions from measured residual elastic strains using the minimization of a quadratic mismatch functional.

The eigenstrain incorporates inelastic strain of any origin: creep and plasticity, mismatch in thermal expansion, structural transformation causing strain, etc. The concept of eigenstrain that serves as the source of residual stress is not in itself novel – for example, Mindlin and Cheng [8] introduced the notion of *nuclei of strain* that clearly signified point eigenstrain causing an equilibrated and concentrated state of self-stress within an elastic body. The main thrust of the research effort on eigenstrain analysis [5, 9, 10] of complex residual stress states undertaken by one of the present authors in recent years [4, 11] is to develop this methodology into a state-of-the-art technique for the characterization and modelling of the consequences of various processing operations, such as surface machining, shot peening [3], welding [7], and heat treatment.

In the eigenstrain model implementation the small-strain-deformation theory is followed. Strain decomposition into elastic and inelastic parts is assumed possible according to

$$\varepsilon_{\text{total}} = e + \varepsilon^*$$

Here $\varepsilon_{\text{total}}$ refers to the total strain, e to the elastic strain, and ε^* to the eigenstrain.

The strategy of solution employed in the subsequent analysis is similar to that used in an earlier publication on eigenstrain analysis of machined plates [4]. Regularization of the inverse problem described in more detail elsewhere [7] consists of representing the unknown continuous eigenstrain distribution (which possesses an infinite number of degrees of freedom) in terms of a linear combination of continuous or discrete basis functions. This formulation, for any fixed number of chosen basis functions, can be shown to guarantee the existence and uniqueness of solution. Representing unknown eigenstrain distributions in the form of

truncated series of modal contributions according to

$$\varepsilon_{ij}^*(\mathbf{x}) = \sum_{k=0}^n a_k^{ij} M_k(\mathbf{x}) \quad (2)$$

reduces the problem to the determination of a finite number n of unknown coefficients a_k^{ij} that ensure the 'best' (in terms of sum-of-squares measure) agreement between the model and experiment. The eigenstrain finite element approach is implemented within the commercial package ABAQUS, although the procedure can be performed with any finite element package.

Other approaches to the problem of reconstruction of residual stress can be noted. The contour method [12] relies on precise measurement of out-of-plane distortion of a carefully cut (e.g. by spark erosion) section surface, and restoring the surface to flat by applying equal and opposite displacement within a finite element model of the object. Although this approach has been applied with some considerable success, it possesses some limitations. For example, the contour method is incapable of reconstructing residual stresses that arise owing to pure shear deformation without out-of-plane displacement, such as after plastic torsion of a circular shaft. The sensitivity of the method is limited to local residual stresses within the section plane.

High-energy X-ray diffraction methods offer the advantages of being non-destructive and achieving high penetration depth in solid structural engineering components [13]. The use of a white beam in combination with an energy-dispersive detector leads to a particularly fast and efficient measurement of bulk residual elastic strains [14]. The interpretation of diffraction patterns containing multiple peaks has been shown to provide an excellent measure of average macroscopic strain [15]. One of the present authors and co-workers [16] have contributed to the development of techniques for the interpretation of experimental results obtained using high-energy synchrotron X-ray diffraction in the white-beam mode. These methods were used in the present study.

Conventional laboratory methods for diffraction stress evaluation rely on the use of relatively low-energy monochromatic radiation and have been used with some significant success to extract depth profile information [17]. However, depth profiling in this case requires electrochemical layer removal and only remains reliable for stress evaluation provided that the etch depth does not exceed fractions of a millimetre. This observation suggests that laboratory (low-energy monochromatic) and synchrotron (high-energy white-beam) techniques possess certain complementarity in the context of

the present problem, i.e. the former delivers highly spatially resolved information (down to 5–10 μm) about near-surface residual stresses, whereas the latter can provide a relatively lower-resolution measure (down to about 30 μm , although further reduction to the micron scale is possible) of the *residual elastic strains* across the entire thickness of the component. In the present study, both methods are used to develop insight into the permanent inelastic strains (eigenstrains) arising in the vicinity of machined surfaces in nickel superalloys.

The fundamental difference between the analysis presented here and the previous investigation described in reference [4] consists of the incorporation of the experimental data obtained from two different cross-sections of the machined plate.

3 EXPERIMENTAL DETAILS

The material used for this study was nickel-based superalloy IN718 with the nominal composition given in Table 1.

The microstructure of the material was analysed using scanning electron microscopy with EBSD, providing the capability for determining grain size and orientation (Fig. 1). Knowledge of the grain structure and grain size distribution is necessary to justify the use of diffraction measurement techniques for the evaluation of *macroscopic* residual stresses and residual elastic strains that must reflect values averaged over representative material volumes. Figure 1 illustrates that sampling volumes of 1000 μm^3 or more ought to be used to collect representative diffraction data. This requirement was observed in all experiments described below.

Superalloy plate was machined under standard conditions used in the manufacture of combustion chamber components. A coupon was then extracted from the plate with the dimensions shown in Fig. 2. Within the coupon the appearance of machined surface was uniform, suggesting that the eigenstrain distributions introduced by the cutting process are likely to remain consistent over the entire area of the

Table 1 Nominal composition of IN718 nickel superalloy

Element	Amount (wt %)
Ni	57
Fe	19
Cr	18
Nb	5
Balance	5

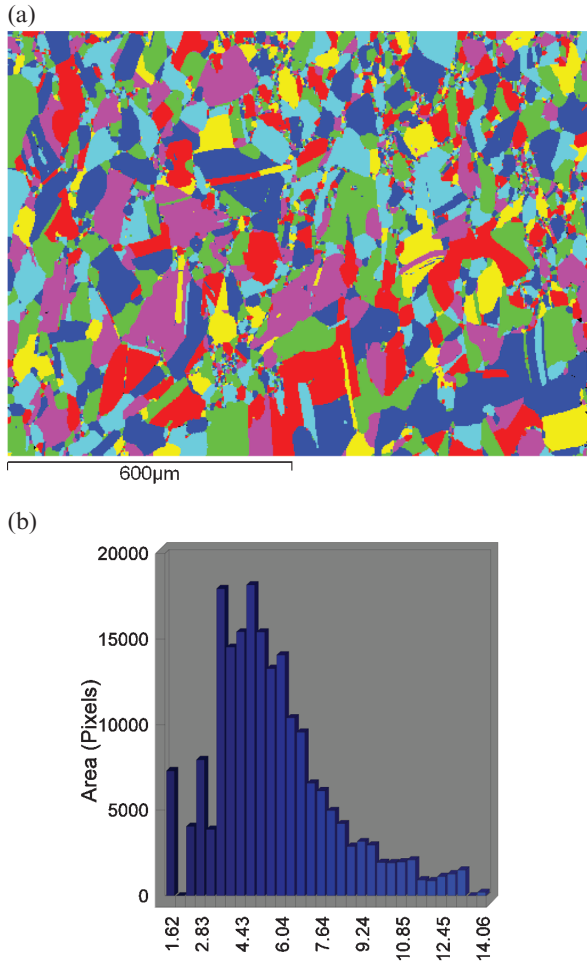


Fig. 1 (a) Illustration of morphology (shapes) and orientation (colours) of crystallite constituents of the nickel superalloy considered in this study. (b) Grain area distribution function represented in terms of area measured in squared pixels. The linear pixel size for the image in (a) was about 2 μm

coupon. Note, however, that the same statement cannot be made concerning the residual stress state which is sensitive to the boundary conditions and therefore relaxes as the edges of the coupon are approached.

Laboratory residual stress measurements were carried out on coupons of nickel superalloy (prior to parting off the slices; see below) in the near-reflection scattering geometry using lower-energy (around 8 keV) monochromatic radiation. A Bruker D8 laboratory X-ray diffractometer was used to collect the data, and the $\sin^2 \psi$ method was employed for residual stress calculation (see, for example, reference [17]). If a continuum elasticity view of residual stress is adopted, i.e. the inhomogeneous anisotropic nature of the polycrystalline aggregate is ignored, then the strain value $\varepsilon_{\varphi\psi}$ depends on the

angles (φ, ψ) illustrated in Fig. 3. The relationship between stresses and strains is given by

$$\begin{aligned} \varepsilon_{\varphi\psi} = & \frac{1}{2}s_2[\sigma_{11} \cos^2 \varphi + \sigma_{12} \sin(2\varphi) + \sigma_{22} \sin^2 \varphi] \sin^2 \psi \\ & + \frac{1}{2}s_2\sigma_{33} \cos^2 \psi + s_1(\sigma_{11} + \sigma_{22} + \sigma_{33}) \\ & + \frac{1}{2}s_2[\sigma_{13} \cos \varphi + \sigma_{23} \sin \varphi] \sin(2\psi) \end{aligned} \quad (3)$$

The stress components σ_{ij} refer to the sample-related axes P11, P22, and P33 indicated in Fig. 3. The coefficients s_1 and s_2 are known as the diffraction elastic constants (DECs). They are related to the elastic compliance of the material and have units of reciprocal gigapascals.

By evaluating the strains $\varepsilon_{\varphi\psi}$ for a sufficient number of angles (φ, ψ) it is possible, in principle, to find the unknown stresses σ_{ij} through least-squares fitting.

In practice the above formula is usually drastically simplified by assuming that the strain measurement is performed at the sample surface. This assumption is likely to be valid for the very shallow beam penetration of several microns. Consequently all stress components σ_{i3} vanish in the above formula.

The orientation of the principal stresses in the plane of the sample surface is frequently known *a priori*. For example, for machined surfaces the principal stresses are likely to be associated with the cutting direction, and the direction perpendicular to it. It is therefore possible to assume that the angle φ in the above formula is equal either to zero or to 90° .

As a result of these simplifications the formula for the strain in terms of stresses is reduced to

$$\varepsilon_{\alpha\alpha}(\psi) = \frac{1}{2}s_2\sigma_{\alpha\alpha} \sin^2 \psi + s_1(\sigma_{11} + \sigma_{22}) \quad (4)$$

where α refers to either component 1 or component 2. It is clear from the above formula that the stress components σ_{11} and σ_{22} can be found from the slope of the plot of $\varepsilon_{xx}(\psi)$ against $\sin^2 \psi$, provided that the DEC s_2 is known.

It is perhaps relevant here to make a note on the limits of validity of continuum elasticity assumptions and the $\sin^2 \psi$ method of analysis. Firstly, owing to the nature of the (monochromatic) diffraction experiment, only a subset of alloy grains are interrogated at each value of the tilt angle ψ , and this subset is in fact different for each angle ψ . This violates the assumption that underlies equation (5), namely that diffraction measurements performed at different angles all probe the stress (strain) state within the same material.

Secondly, the measured strain within the diffracting grain subset may not be representative of the overall macroscopic average elastic strain within the polycrystalline aggregate. In fact, because of the inhomogeneity and anisotropy of the elastic and

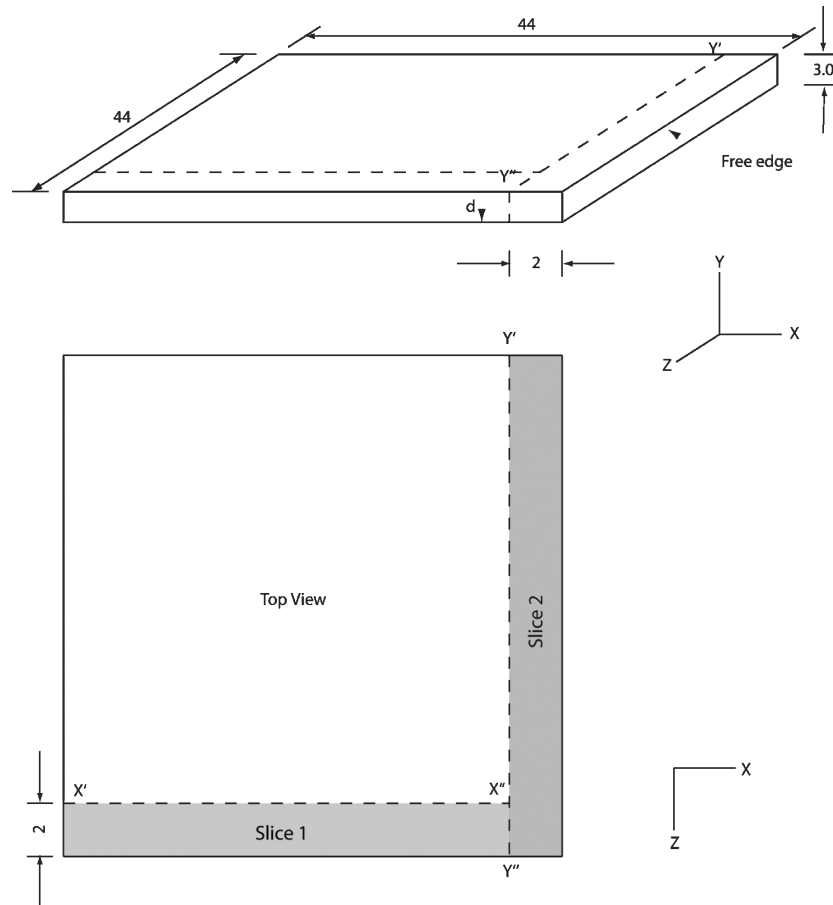


Fig. 2 Illustration of the geometry of the coupon from surface-machined nickel superalloy IN718 plate analysed by X-ray diffraction

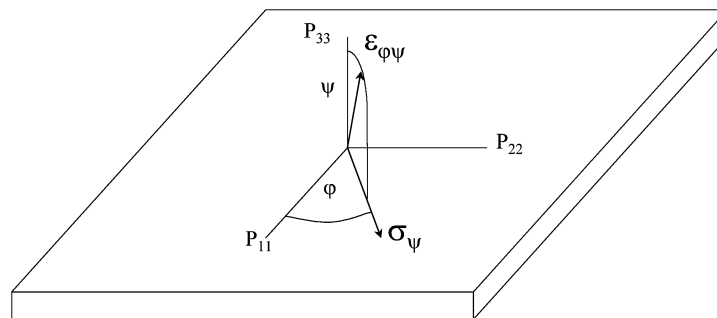


Fig. 3 The orientation of strain measurement direction (the scattering vector) with respect to the sample surface, defined using the angles φ and ψ

plastic properties of real crystals the deformation of grain subsets is strongly sensitive to orientation both in the laboratory coordinate system (i.e. with respect to the loading directions in the sample) and in the crystal coordinate system (i.e. in terms of the Miller indices of the reflection). Furthermore, the linear relationship between the strain $\varepsilon_{\alpha\alpha}(\psi)$ and $\sin^2 \psi$ is unlikely to persist in the presence of significant grain level plastic deformation for the strain based on an arbitrary hkl diffraction peak. For these reasons the

choice of the diffraction peak for residual stress determination using the $\sin^2 \psi$ technique must be made judiciously.

Substantial experimental and theoretical studies have been dedicated to the analysis of polycrystalline deformation, and the selection of the most suitable hkl diffraction peaks for strain measurement using neutron diffraction [18]. However, the selection of diffraction peaks for the $\sin^2 \psi$ analysis, surprisingly, does not seem to have received a similar amount of

attention. The report in reference [19] uses elasto-plastic self-consistent analysis to provide justification for the selection of the 311 diffraction peak for bulk residual stress analysis in nickel superalloy components. This corresponds to the Bragg scattering angle of approximately 145° in Cu $K\alpha$ radiation.

Because of the extremely shallow depth of penetration of the low-energy X-rays, laboratory diffraction studies are typically confined to the very near surface (about $10\text{ }\mu\text{m}$) layers of material. Depth profiling is, however, possible by using chemical layer removal techniques (etching with acid solution) [19].

Two slices, designated slice 1 (cut along section $X'-X''$) and slice 2 (cut along section $Y'-Y''$) were detached from the coupon using slow setting of an electric discharge machining (EDM) tool. The motivation for choosing EDM is to use a cut that introduces as little disturbance as possible to the pre-existing eigenstrain state. The resulting slices were studied using high-energy synchrotron X-ray scattering.

Diffraction strain measurements were carried out on Station 16.3 at the Synchrotron Radiation Source, Daresbury, UK. Measurements were carried out in the white-beam energy-dispersive mode in transmission through the slices, i.e. with the incident X-ray beam initially travelling in the positive z direction for slice 1, and in the x direction for slice 2. Scanning of the beam was performed in the plane normal to the incident beam direction, i.e. in the x - y plane for slice 1, and the y - z plane for slice 2. The detector was offset at a small angle of about 12° with respect to the incident beam within the diffraction plane. The slices were then tilted by an angle of 6° around the y axis, to ensure that the scattering vector direction coincided with one of the in-plane directions of the slices.

The prime interest in the current study is the residual strain component parallel to the machined surface of the slice, i.e. the x direction in slice 1, and the z direction in slice 2. Since slicing primarily relieves the strains in the direction perpendicular to the cut, this measurement arrangement ensured that good measurement sensitivity could be achieved for strain component ε_{xx} in slice 1, and strain component ε_{zz} in slice 2. The data were then combined in the eigenstrain analysis to obtain a full three-dimensional reconstruction of the residual elastic strain state.

The incident beam was defined through two pairs of crossed slits that were open 0.1 mm wide parallel to the machined surface of the slice, and 0.025 mm wide in the direction normal to the machined surface, to deliver high spatial resolution in the direction of rapid variation in the residual strain.

Diffraction patterns containing at least five diffraction peaks of nickel were collected in the white-beam mode. The detector channel-to-energy conversion characteristic was assumed to be parabolic, and calibrated using the diffraction pattern from the National Bureau of Standards silicon powder standard, and the procedure described by Liu *et al.* [16]. A series of diffraction patterns was taken along the lines perpendicular to the machined surface, with the step of 0.025 mm across the entire samples, until the sampling volume emerged from the specimen on the opposite side.

The strain-free value of lattice parameter was evaluated by performing a measurement on a stress-relieved gauge volume of material corresponding to the corner of the slice. It was found from subsequent stress reconstruction analysis that this reference lattice spacing value was indeed consistent with the requirement of static equilibrium. The measured residual elastic strain profiles are illustrated in Figs 4 and 5 by open circles and are discussed below.

4 RESULTS

In the present study the interest is focused on the through-thickness variation in the unknown eigenstrain distributions $\varepsilon_{xx}^*(y)$ and $\varepsilon_{zz}^*(y)$ parallel to the machined surface. While the eigenstrain component ε_{yy}^* normal to the machined surface may also be present in the sample, simulations reveal that its influence on the residual elastic strain and stress state is insignificant [4]. While in the previous study [4] it was assumed that the two eigenstrain components ε_{xx}^* and ε_{zz}^* parallel to the machined surface were equal to each other, this restriction is lifted in the present analysis. In fact, the purpose of the present experimental and modelling investigation is to reveal whether significant differences exist between the results obtained if this assumption is enforced, or otherwise.

Furthermore, in the previous investigation the eigenstrain distribution was assumed to be confined to the relatively thin near-surface region. Synchrotron X-ray diffraction measurements reveal, however, that residual elastic strain variation persists throughout the specimens.

Since the eigenstrain distributions are assumed to vary with the depth y from the machined surface, the scaled variable ς is introduced as follows: $\varsigma = (2y - t)/t$, so that $-1 \leq \varsigma \leq 1$ as $0 \leq y \leq t$, where t is the sample thickness. A series of Chebyshev polynomials of the first kind given by

$$T_k(\varsigma) = \cos k \arccos(\varsigma) \quad (5)$$

is used to express $\varepsilon_{xx}^*(y)$ and $\varepsilon_{zz}^*(y)$ using $M_k(\mathbf{x}) = T_k(\zeta)$ in equation (2), so that

$$\varepsilon_{xx}^*(y) = \sum_{k=0}^n a_k T_k(\zeta), \quad \varepsilon_{zz}^*(y) = \sum_{k=0}^n b_k T_k(\zeta) \quad (6)$$

In the above expressions a_k and b_k denote the sets of coefficients to be determined by the variational procedure [3], and n is the number of terms in the series.

For the purposes of the analysis articulated above, eigenstrain distributions were determined for *three* different models, as follows.

Case 1. This case consists of the two-dimensional model of slice 1 due to $\varepsilon_{xx}^*(y)$, but ignoring the presence of $\varepsilon_{zz}^*(y)$.

Case 2. This case consists of the two-dimensional model of slice 2 due to $\varepsilon_{zz}^*(y)$, but ignoring the presence of $\varepsilon_{xx}^*(y)$.

Case 3. This case consists of the three-dimensional model of a plate due to both $\varepsilon_{zz}^*(y)$ and $\varepsilon_{xx}^*(y)$.

The elastic strain distributions arising owing to eigenstrain terms were calculated using reduced two-dimensional and fully three-dimensional finite element analyses. The relationship between the deformation states in the coupons (slices) and the entire object is of primary interest in the present study and will be discussed in detail in the next section.

Figure 4(a) presents the comparison between experimental residual strain data (open circles) and the calculated prediction for residual elastic strain $e_{xx}(y)$ using case 1 formulated above. The corresponding residual stress $\sigma_{xx}(y)$ distribution in the slice is illustrated in Fig. 4(b). In this example the number of terms in the series in equation (6) was $n = 15$, which was found to be sufficient to capture the details of residual elastic strain variation in the sample.

Figure 5(a) presents a similar comparison between experimental residual strain data (open circles) and the calculated prediction for residual elastic strain $e_{zz}(y)$ using case 2. The corresponding residual

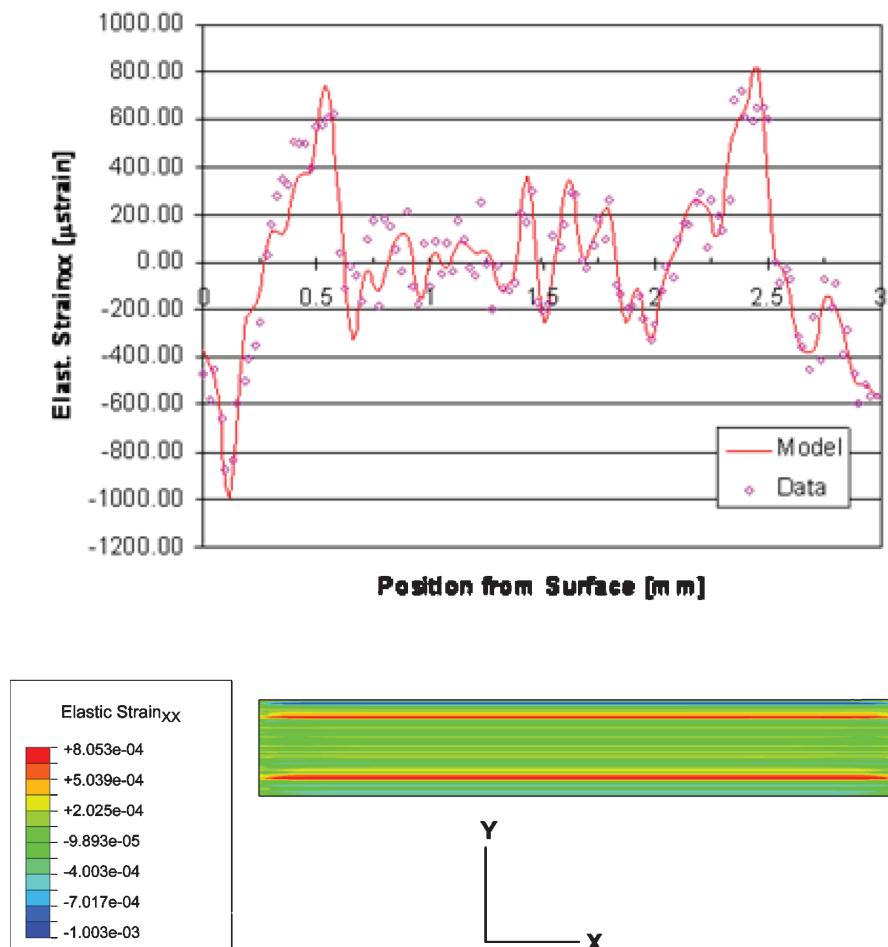


Fig. 4 Slice 1 experimental measurements and two-dimensional reconstruction results

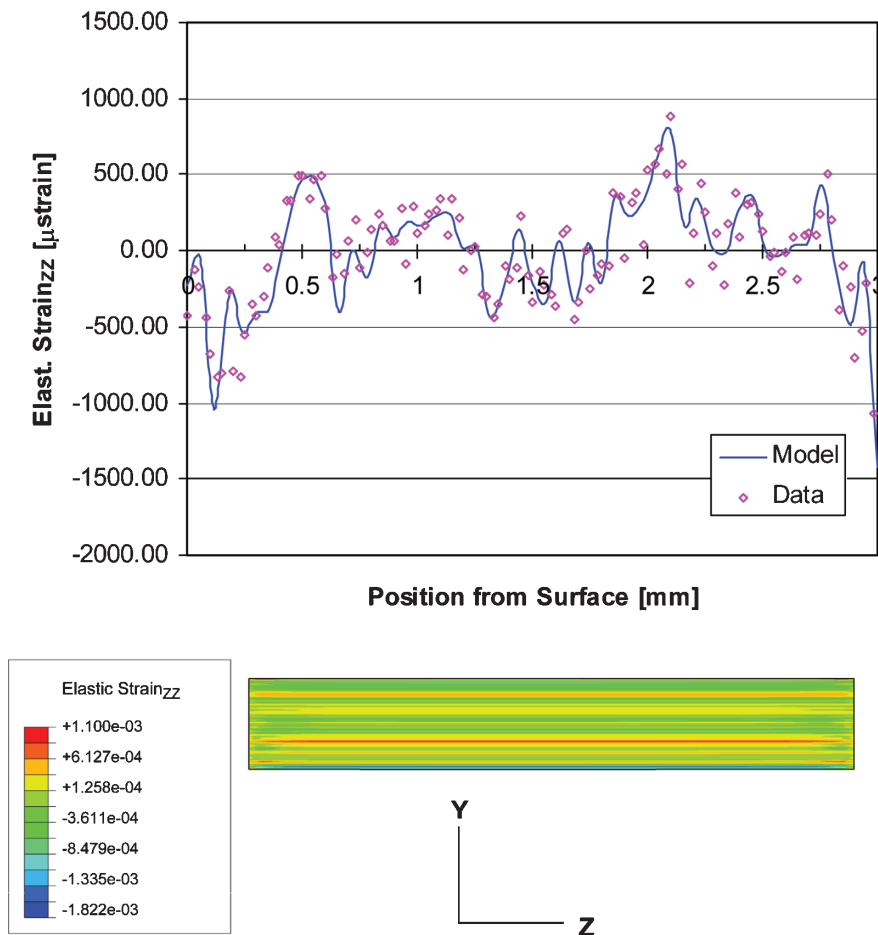


Fig. 5 Slice 2 experimental measurements and two-dimensional reconstruction results

stress $\sigma_{zz}(y)$ distribution in the slice is shown in Fig. 5(b).

A particular note should be made about the nature of residual elastic strain distribution within the nickel superalloy slices considered in the present study. The coupons were extracted from a ring-rolled forging that had undergone significant plastic deformation prior to surface machining. As a consequence, the test pieces retain 'memory' of this processing operation in the form of permanent inelastic (plastic) strains that are particularly prominent close to the middle of the slices. These residual strains are highly scattered, as might be expected owing to the relatively larger grain size observed in this region. Although the use of white-beam X-ray diffraction and multiple-diffraction-peak analysis provides the best approximation for the 'true' value of macroscopic average residual elastic strain, it is impossible to exclude the influence of finite sampling, particularly under the conditions when the scattering volume is relatively small, and the grain size relatively large.

In contrast, close to the surface of the slices the residual elastic strain profiles are dominated by the

consequence of surface machining. The resulting deformation pattern within the nickel superalloy material subjected to cutting is dominated by shear, leading to grain refinement and residual shearing plastic strain parallel to the machining direction. The detailed nature of the very-near-surface residual stress state was investigated with the help of laboratory X-ray diffraction using the $\sin^2 \psi$ method of analysis and will be described below.

Now attention is turned, once again, to the subject of residual stress reconstruction within the coupon based on the information collected from synchrotron diffraction measurements. Eigenstrain-based reconstruction analyses of residual stress for case 1 and case 2 described above were carried out by neglecting the simultaneous presence of eigenstrains $\epsilon_{xx}^*(y)$ and $\epsilon_{zz}^*(y)$. In case 3 the coupled problem is tackled, when both $\epsilon_{xx}^*(y)$ and $\epsilon_{zz}^*(y)$ are considered to be present, and both residual elastic strain component profiles $e_{xx}(y)$ and $e_{zz}(y)$ are matched using the variational procedure. Figures 6(a) and (b) illustrate the results of this analysis, in comparison with the reconstructions previously obtained in case

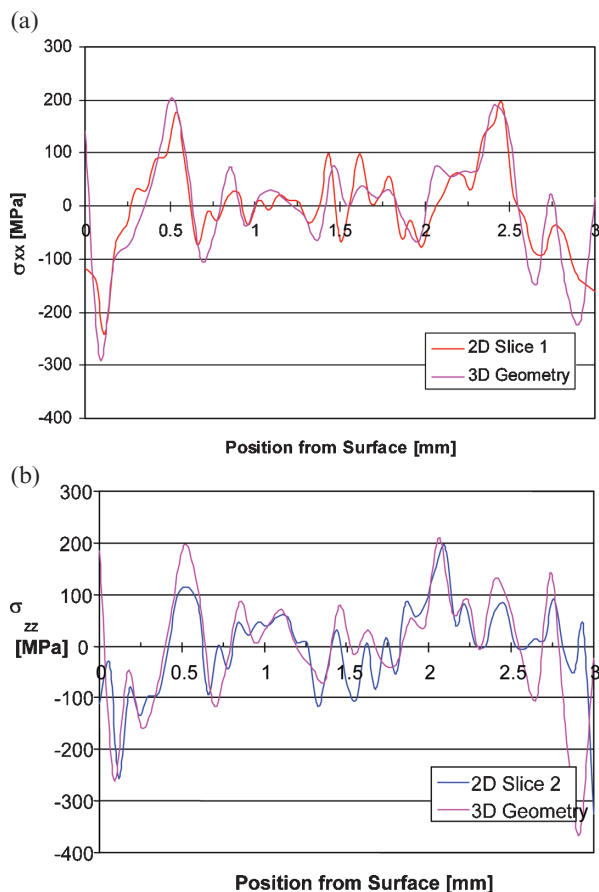


Fig. 6 The result of three-dimensional (3D) reconstruction of residual stress based on coupled analysis of the same experimental results used previously for one-dimensional analyses. For comparison the results from the two-dimensional (2D) reconstructions obtained in (a) case 1 and (b) case 2 are also included

1 and case 2 respectively. It is apparent that the difference between the two approaches is relatively small, although substantial differences are observed in some regions.

It should be noted that eigenstrain analysis essentially corresponds to elastic continuum theory perturbed by the presence of permanent incompatible strains. Therefore, the amount of coupling between components, i.e. the influence of $\epsilon_{xx}^*(y)$ on $e_{zz}(y)$, and of $\epsilon_{zz}^*(y)$ on $e_{xx}(y)$, is scaled by the magnitude of Poisson's ratio, compared with the direct influence of $\epsilon_{xx}^*(y)$ on $e_{xx}(y)$, and of $\epsilon_{zz}^*(y)$ on $e_{zz}(y)$.

The level of detail of residual stress reconstruction in the very-near-surface regions may be insufficient for the purposes of precise analysis of fatigue crack initiation, particularly if the effects of stress gradients are to be taken into account. For this reason the results may be usefully supplemented by laboratory X-ray diffraction measurements with chemical surface

removal, which may provide spatial resolution down to about 10 μm .

Figure 7(a) illustrates the very-near-surface residual stress profiles obtained by chemical etching for the stress components along and perpendicular to the machining direction. Some significant differences between the two components should be noted. At the very surface of the machined piece, one component is tensile, while the other is compressive. Both stress components become more compressive at very shallow depths and reach their most compressive values only at about 10 μm below the machined surface. Beyond that depth both components show a gradual reduction in the magnitude of compressive residual stress.

If the two measured residual stress components, along the machining direction and perpendicular to it, are assumed to be the principal in plane stresses, then half of the difference between them represents the largest in plane residual shear stress in the machined surface. Figure 7(b) shows the result of this

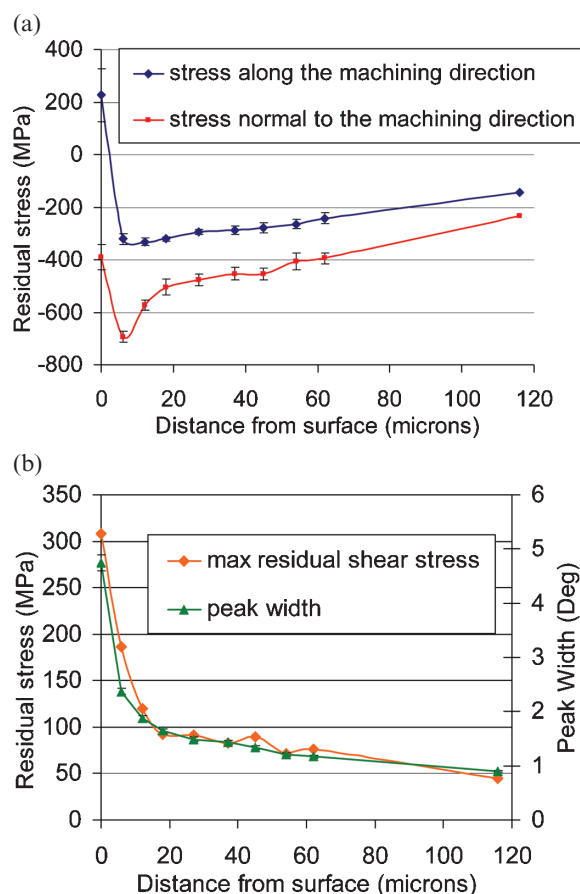


Fig. 7 (a) Depth profiles of residual stresses along (σ_{xx}) and normal (σ_{zz}) to the machining direction. (b) Comparison between the maximum residual shear stress and plasticity-induced peak broadening

simple calculation, together with the diffraction peak width that is representative of the amount of plasticity induced in the surface. The agreement between the two profiles is quite striking and suggests a common origin of the two independent measures of machining-induced plasticity. These measurements thus substantiate the hypothesis that very-near-surface residual stresses in machined components are produced by plastic shearing during metal cutting.

5 DISCUSSION

The analysis of residual stresses and residual deformation (eigenstrains) in the vicinity of machined surfaces is an important topic of interdisciplinary research, in that it has direct relevance to manufacturing and process modelling, numerical simulation of complex deformation behaviour accompanied by hardening, damage and material failure, and residual stress measurement and analysis. The state of permanent deformation and residual stresses arising within the material changes as a consequence of machining using different process conditions (feeds, speeds, cutting angles, etc.) Understanding the nature of residual stresses arising as a consequence of machining may be conveniently achieved in terms of eigenstrain distributions. These distributions in turn can be parameterized to reduce the number of degrees of freedom required for the description. The final task is to establish the relationships between these eigenstrain-based descriptions of the *consequences* of machining, and the *machining conditions* themselves.

Several obstacles present themselves on this path. Firstly, permanent deformations induced by machining are usually localized within very thin near-surface layers. Therefore, their characterization requires appropriately high spatial resolution. Furthermore, machining is usually carried out on objects that have prior processing history, such as the objects considered in the present study that consist of thin shells machined from ring-rolled forgings. If the entire residual stress or residual elastic strain state is interrogated, it will almost invariably be found that machining-induced permanent strains are superimposed on previously existing eigenstrains created by plastic deformation, or heat treatment, or some other processing operation.

A particularly intriguing question concerns the comparative magnitude and significance of machining-induced eigenstrains *vis-à-vis* those introduced by prior plastic bending. It is possible to argue that plastic strains developed during machining must

correspond to the large amounts of deformation that a material can sustain just before failure, since machining ultimately involves material separation [2]. This might be thought to imply that eigenstrain values might also be particularly high.

It should be noted, however, that eigenstrains are not simply equivalent to total permanent inelastic strains. The distinction can be clearly seen if uniform stable stretching of a solid bar is considered. Even after significant permanent plastic strain has been achieved, no macroscopic residual stress will be found upon unloading, and hence no active eigenstrain will be present in the bar. In other words, eigenstrain magnitude does not simply scale with the amount of plasticity experienced by the material volume. It rather relates to the mismatch between this volume and its neighbours, or to the local value of the plastic strain gradient.

The analysis could be carried out further to argue that high magnitudes of the plastic strain gradient are likely to be induced by machining in the presence of high local shear tractions. In fact, the experimental observations presented in the current study suggest that machining-induced plasticity overcomes the pre-existing residual stress state, thus 'erasing material memory' of prior plasticity. For this reason the near-surface residual stress states in machined components are dominated by the consequences of machining, rather than by prior plastic deformation. The situation is reversed within the bulk of the object, where the effects of surface machining are not significant, and residual stresses reflect the consequences of earlier stages of processing involving bulk plastic deformation, recrystallization during heat treatment, etc.

The ultimate aim of eigenstrain modelling activity, in the present authors' opinion, is to develop a continuum of methods that incorporates processing analysis, component characterization, and residual stress analysis, ultimately feeding into fatigue life prediction methods for the purposes of engineering design. Although clearly this goal cannot be attained in any single paper, it is hoped that the present study contributes a step in this direction.

6 CONCLUSION

Variational eigenstrain procedures for the reconstruction of residual stress described above can be successfully applied to three-dimensional models of slices partitioned off from a machined nickel plate. Elastic residual strains were reconstructed first by ignoring the coupling between the two in-plane

eigenstrain and strain components, and then within a three-dimensional model that allowed for the simultaneous influence of the two components, each of which varied through the thickness.

The residual strain distributions indicate the presence of permanent deformations inherited by the system from different processing operations. In particular, the regions of the sample lying close to the midthickness display some scatter associated with the ring-roll forging operation. On the other hand, the regions lying close to the sample's machined surfaces show residual stress distributions induced by metal cutting.

The detailed near-surface residual stress distributions were further analysed at high through-thickness resolution using laboratory X-ray diffraction in combination with chemical layer removal. An interesting correlation has been established between the maximum residual in-plane shear stress, and plasticity-induced diffraction peak broadening. This correlation suggests that the very-near-surface residual stress state is induced by material shearing deformation during cutting.

REFERENCES

- 1 Rohde, U. and Jeppsson, A. Literature review of heat treatment simulations with respect to phase transformation, residual stresses and distortion. *Scand. J. Metall.*, 2000, **29**, 47–62.
- 2 Atkins, A. G. Rosenhain and Sturkey revisited: the 'tear' chip in cutting interpreted in terms of modern ductile fracture mechanics. *Proc. Instn Mech. Engrs, Part C: J. Mechanical Engineering Science*, 2004, **218**, 1181–1194.
- 3 Korsunsky, A. M. On the modelling of residual stresses due to surface peening using eigenstrain distributions. *J. Strain Analysis*, 2005, **40**(8), 817–824.
- 4 Korsunsky, A. M., Regino, G. M., Latham, D., Liu, J., Nowell, D., and Walsh, M. J. Eigenstrain analysis of synchrotron X-ray diffraction measurement of residual strains in machined nickel alloy plates. *J. Strain Analysis*, 2006, **41**(5), 381–395.
- 5 Mura, T. *Micromechanics of defects in solids*, 1987 (Martinus Nijhoff, Dordrecht).
- 6 Korsunsky, A. M. On the use of interpolative quadratures for hypersingular integrals in fracture mechanics. *Proc. R. Soc. A*, 2002, **458**(2027), 2721–2733.
- 7 Korsunsky, A. M., Regino, G., and Nowell, D. Variational determination of eigenstrain sources of residual stress. In Proceedings of the International Conference on *Computational and Experimental Engineering Science* (ICCES 2004), 26–29 July 2004 (Eds A. J. B. Tadeu and S. N. Atluri).
- 8 Mindlin, R. D. and Cheng, D. H. Nuclei of strain in the semi-infinite solid. *J. Appl. Phys.*, 1950, **21**, 926–930.
- 9 Ueda, Y., Fukuda, K., and Kim, Y. C. New measuring method of axisymmetric three-dimensional residual stresses using inherent strains as parameters. *Trans. ASME*, 1986, **108**, 328–334.
- 10 Ueda, Y. and Yuan, M. G. Prediction of residual stresses in butt welded plates using inherent strains. *J. Engng Mater. Technol.*, 1993, **115**, 417–423.
- 11 Korsunsky, A. M. Residual elastic strain due to laser shock peening: modelling by eigenstrain distribution. *J. Strain Analysis*, 2006, **41**(3), 195–204.
- 12 Prime, M. B., Sebring, R. J., Edwards, J. M., Hughes, D. J., and Webster, P. J. Laser surface-contouring and spline data-smoothing for residual stress measurement. *Expl Mechanics*, 2004, **44**, 176–184.
- 13 Korsunsky, A. M., Wells, K. E., and Withers, P. J. Mapping two-dimensional state of strain using synchrotron X-ray diffraction. *Scripta Materialia*, 1998, **39**(12), 1705–1712.
- 14 Korsunsky, A. M., Collins, S. P., Owen, R. A., Daymond, M. R., Achtioui, S., and James, K. E. Fast residual stress mapping using energy-dispersive synchrotron X-ray diffraction on station 16.3 at the SRS. *J. Synchrotron Radiation*, 2002, **9**, 77–81.
- 15 Daymond, M. R. The determination of a continuum mechanics equivalent elastic strain from the analysis of multiple diffraction peaks. *J. Appl. Phys.*, 2004, **96**(8), 4263–4272.
- 16 Liu, J., Kim, K., Golshan, M., Laundry, D., and Korsunsky, A. M. Energy calibration and full-pattern refinement for strain analysis using energy-dispersive and monochromatic X-ray diffraction. *J. Appl. Crystallogr.*, 2005, **38**, 661–667.
- 17 Prevey, P. S. X-ray diffraction residual stress techniques in *Metals handbook*, Vol. 10, 1986, pp. 380–392 (American Society for Metals, Metals Park, Ohio).
- 18 Clausen, B., Leffers, T., and Lorentzen, T. On the proper selection of reflections for the measurement of bulk residual stresses by diffraction methods. *Acta Materialia*, 2003, **51**, 6181–6188.
- 19 Korsunsky, A. M. and James, K. E. Measurement of near-surface residual stress on coupons from forged and machined combustor casings. Report, Rolls-Royce University Technology Centre in Solid Mechanics, University of Oxford, 2002, 36 pp.